ICIC Express Letters
Part B: Applications
Volume **7**, Number **2**, February **2016**

 ISSN 2185-2766
pp. 455–460

RESEARCH ON THE DYNAMIC EVOLUTION OF COAL MINING SUBSIDENCE AREAS BASED ON REMOTE SENSING IMAGING

Yujuan Zhang[1] and Ming Huang[2,*]

[1]School of Forestry
Northeast Forestry University
No. 26, Hexing Road, Xiangfang District, Harbin 150040, P. R. China
zyjamy@126.com

[2]Key Laboratory for Urban Geomatics of National Administration
of Surveying, Mapping and Geoinformation
Beijing University of Civil Engineering and Architecture
No. 1, Zhanlanguan Road, Xicheng District, Beijing 100044, P. R. China
*Corresponding author: huangming@bucea.edu.cn

Received October 2015; accepted December 2015

Abstract. *About the quantitative analysis of coal mining subsidence areas, this paper discusses utilization of multi-temporal and multi-sensor remote sensing imaging to achieve the dynamic evolution analysis of monitoring coal mining subsidence areas. The method is to conduct geometric correction and geographic location registration on selected aerial photographs, TM\ETM, SPOT1 and SPOT5 images, to improve the interpretation ability of remote sensing imaging through the method of data fusion based on the spectral fidelity of constant energy principles, and to adopt the secondary fusion processing of digital terrain information and remote sensing imaging to gain a comparative analysis of the scopes and causes of the distribution change in subsidence areas at different times. The test showed that data fusion based on the spectral fidelity of constant energy principles and the secondary fusion method of digital terrain information and remote sensing imaging could accurately depict the dynamic evolution process of coal mining subsidence areas.*

Keywords: Subsidence areas, Remote sensing image, Spectral fidelity, Image fusion

1. **Introduction.** The environmental geological effect caused by coal mining in mining areas is the most noticeable ground surface subsidence in goaves, where the impact is long-term and complicated. It not only renders a great deal of land resources unable for use every year, but also jeopardizes surface buildings, which results in great losses. At present, the main monitoring method in coal mining subsidence areas is to lay the surface movement observation stations above the working surfaces, and adopt leveling and GPS surveying to regularly observe the surface subsidence and horizontal movement caused by mining. This method is only suitable for monitoring the movement and deformation of small areas, and unable to satisfy the large-scale monitoring tasks of diggings. In addition, this method requires significant workloads and is unable to intuitively and conveniently reflect the distribution of ground surface subsidence. Meanwhile, this method is one kind of point measurement, from which it is difficult to obtain the panoramic distribution information of continuous space coverage.

Satellite remote sensing imaging possesses macroscopic, objective, comprehensive, dynamic and rapid characteristics. Using the Huainan Mining Area as a pilot, this research carries out remote sensing surveying and monitoring regarding coal mining subsidence, which aims at obtaining the dynamic change information of subsidence areas, providing a scientific basis for developing the reclamation and governance of subsidence areas as well as the restoration and reconstruction of the ground surface eco-environment. The

utilization of remote sensing technology in diggings has experienced development from early aerial remote sensing to current satellite remote sensing. Many domestic scholars, including Sheng et al. (2001) [1], Peng et al. (2002) [2], Chen (2003) [3], Chen et al. (2004) [4], Hu et al. (2005) [5], Wu and Shi (2004) [6], Ma et al. (2011) [7], Li et al. (2014) [8], respectively utilized aerial and satellite imaging, ERS-1/2 radar data of coal mining areas to conduct environmental monitoring and eco-environment surveying. Many researches showed that each phase distribution and precise scope of the subsidence area can be extracted easily by processing and analyzing the multi-temporal high spatial resolution optical images.

2. Remote Sensing Data Processing.

2.1. **Data selection.** The sensing data sources selected by this research include Landsat TM (ETM), SPOT1 (PAN) and SPOT5 (PAN, B-1/2/3/4). Huainan Mining Area is relatively low and there are permanent rivers nearby, and the ground surface subsidence areas have a close relationship with water body distribution. Researchers selected satellite remote sensing imaging from different periods which were in the same season and had relatively stable water body distribution. According to the local meteorological data analysis, the rain is comparatively little and the surface water body is relatively stable in the Huainan Mining Area from December to May. For the sake of contrast analysis, the Landsat TM (ETM) imaging during the above period from different years was selected, and the multi-temporal feature of Landsat and the high-resolution feature of SPOT imaging were used to conduct a coal mining subsidence situation survey.

2.2. **Geometric correction and geographic location registration of imaging.** According to the relationship between remote sensing imaging from different time phases and topographic map coordinates, imaging from different time phases is conducted using geometric correction processing, which enables such processing and geographical position registration among different imaging to be ultimately achieved. Although this process completes two tasks, it actually only requires execution of one-time spatial transformation processing on images. Thus, the loss of imaging information is reduced, which is a better image processing method. Quadratic polynomials are adopted to conduct coordinate transformation, cubic convolutions are used to conduct gray resampling, the matching precision of remote sensing imaging and corresponding scale topographic maps can be within 0.5 pixels (TM/ETM remote sensing imaging and a $1:50,000$ scale topographic map; SPOT5 panchromatic remote sensing imaging and a $1:10,000$ scale topographic map), and mapping deviation of imaging can be controlled within 0.2mm, which means it is essentially able to meet the spatial geometry accuracy requirements of corresponding scales.

2.3. **Image data fusion.** Remote sensing imaging data fusion processing technology can convert the remote sensing imaging of different spatial, spectral and time resolution ratios to the uniform time-space coordinate system with the same spatial resolution ratio, forming a group of new spatial information, namely, fusion into a group of new remote sensing imaging. The fusion technology can perfect the display quality of imaging and improve the interpretation ability of remote sensing imaging. Researchers adopt the following imaging fusion methods [9].

(1) Calculate the average brightness value of the sub-pixels of high-resolution imaging. For the pixel anywhere (x, y) on low-resolution imaging, its corresponding sub-pixels of high-resolution imaging are $(nx + i, ny + j)$ $(i, j = 0, 1, 2, \ldots, n - 1)$, and $n = \frac{Spatial_{Low}}{Spatial_{High}}$ is the spatial resolution ratio of two kinds of imaging. The brightness values of imaging pixels are respectively denoted as $DN_{Low}(x, y)$ and $DN_{High}(nx+i, ny+j)$, and the average

brightness value $\overline{DN}_{High}$ of a group of sub-pixels of high-resolution imaging is calculated in accordance with Equation (1):

$$\overline{DN}_{High}(x,y) = \frac{1}{n^2} \sum_{i=0,j=0}^{i=n-1,j=n-1} DN_{High}(nx+i, ny+j) \tag{1}$$

In the equation, $x, y = 0, 1, 2, 3, \ldots$.

Every pixel on low-resolution imaging has a group of corresponding sub-pixels and the brightness value of the sub-pixels on high-resolution imaging.

(2) Calculate the brightness difference of the pixels on different resolution imaging. Every pixel on low-resolution imaging has a certain brightness difference with the pixel at the corresponding position on high-resolution imaging. This value is a function of pixel position (x, y), and set as $g(x, y)$. Its expression is

$$g(x,y) = DN_{Low}(x,y) - \overline{DN}_{High}(x,y) \tag{2}$$

(3) Summation. Add the brightness difference calculated through Equation (2) to every corresponding sub-pixel on high-resolution imaging, forming a new sub-pixel brightness value.

$$DN'_{High}(nx+i, ny+j) = DN_{High}(nx+i, ny+j) + g(x,y) \tag{3}$$

$\overline{DN'}_{High}(x,y) = DN_{Low}(x,y)$ can be obtained through the deducting process of Equation (3). After fusion, the average brightness value of a group of sub-pixels on imaging equals the brightness value of corresponding pixels on low-resolution imaging; specifically, within the range of one pixel on low-resolution imaging, the spectral energy of fusion and low-resolution images is invariant, and the spectral information gains fidelity. Consequently, the fusion imaging obtained through this method not only keeps the spectral efficiency of low-resolution imaging invariable, but also possesses the spatial features of high-resolution imaging. Figure 1 is TM imaging and the fusion of TM and SPOT1 PAN imaging.

FIGURE 1. TM image and its fusion with SPOT1 PAN image

2.4. **Thematic information processing of remote sensing imaging.** The ground storage in the Huainan Mining Area is shallow. Large-area ponding is the main characteristic of coal mining subsidence areas, and the scope changes of a water body have a close relationship with subsidence changes. Water bodies and subsidence areas [10,11] can be extracted in a relatively accurate fashion through remote sensing imaging classification techniques, and meanwhile, digital terrain information and remote sensing imaging are conducted using fusion processing, so that the two sets of data can be gathered onto one image, which is conducive to conducting a comparative analysis [12-16] on the scopes and causes of water body distribution changes at more than one period, providing actual and objective plane data for the survey in coal mining subsidence areas. Taking the water body distribution diagram discerned by remote sensing imaging in 1994 as an early image,

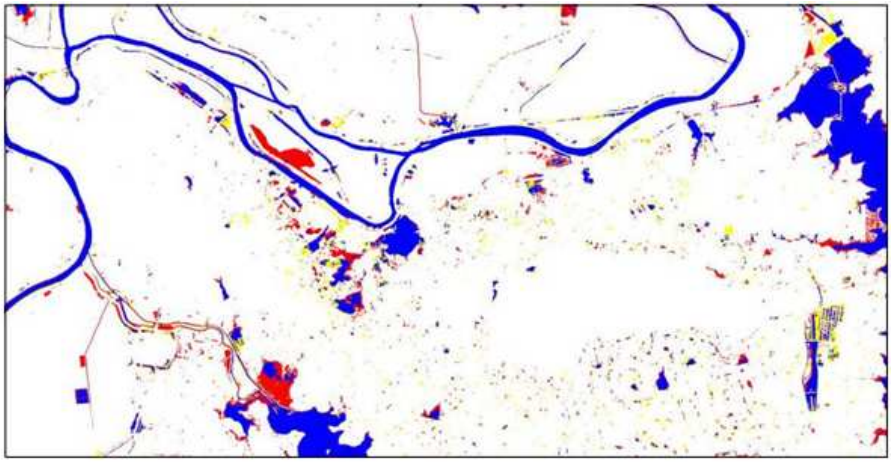

FIGURE 2. Schematic diagram of water body changes in mine from 1994 to 2011

and using the water body distribution diagram discerned by remote sensing imaging in 2011 as the current image, Figure 2 is a fusion image which is generated through feature fusion processing. In the figure, the blue represents comparatively permanent pool zones, the red is newly increased pool zones and the yellow denotes ponding disappearance zones. Figure 2 clearly reflects the water body distribution change situation in the Huainan Mining Area from 1994 to 2011.

3. Remote Sensing Imaging Analysis of Coal Mining Subsidence Areas.

3.1. Current situation and main distribution characteristics of subsidence areas.

By the end of 2011, the area of the coal mining subsidence area of the Huainan Mining Area had reached 50.58km^2, in which the area of subsidence of the west mining area (from the Kongque mine to the Li Yingzi mine) is 37.06km^2, and the area of subsidence of the Jiulong Hill and Datong Mine is 13.52km^2. The data of underground goaves in the Huainan Mining Area are provided by the Huainan Mining Group.

3.2. Kongji Coal Mines – Bagong Mountains – the Cai's Hill Area.

The subarea, whose ranges of longitude and latitude are 116°46′06″E-116°55′54″E and 32°34′51″N-32°42′43″N, is located in the west of the Huainan Mining Area. This area is an important coal mining subsidence area in the Huainan region, and the totality displays irregular distribution with northwest-southeast orientation. Table 1 is the water body distribution change at different periods (taking the water body distribution in 1994 as an early image and taking the water body distribution in other periods as the current image). It can be seen from Table 1 that, when the areas of newly increased pool zones and water body disappearance zones are relatively large, the corresponding times are 2009, 2010 and 2011, which indicates that the water body distribution changes are relatively big during these periods. In consideration of the fact that the water body image in 2009 was gained from remote sensing imaging conducted on July 11th, 2009, and that time was during the rainy season in the Huainan Mining Area, which has a certain difference from the remote sensing imaging during the non-rainy season, they do not have comparability. Therefore, the remote sensing imaging of 2009 is not considered in the contrast analysis of imaging.

Figure 3 is the boundary characteristics fusion image of the remote sensing image of 2011 and the water body distribution change characteristics from 1994 to 2011, in which the white line is the boundary of a relatively permanent pool zone, and the yellow line is the boundary of an impounded surface water disappearance zone. Upon field investigation, it was discovered that most water body disappearance areas corresponded to subsidence landfill areas. For example, the Lizuizi Mining Area (B1) and the Xinzhuangzi Mining

TABLE 1. Water body changes in Kongji and Bagong Mountains and Caijiagang Mine from 1994 to 2011

(unit: pixel)

Time	Other surface feature	Water body disappearance zones	Newly increased pool zones	Relatively permanent pool zones
1994.04	887854	17518	9558	74470
1996.04	876362	12896	21050	79092
1997.04	878663	18749	16437	75551
1997.12	881304	16218	16108	75770
1998.10	878133	20104	19279	71884
2000.04	866012	11743	31400	80245
2001.12	876497	18083	20915	73905
2002.12	877279	22664	20133	69324
2003.12	873471	20806	23941	71182
2004.03	862505	34907	14857	77131
2004.08	866638	23775	30774	68213
2005.04	857676	39736	13079	78909
2005.11	871243	20516	26169	71472
2006.12	866531	30881	17236	74752
2007.04	866531	17236	30881	74752
2008.04	864221	17783	33191	74205
2009.07	858501	27452	38911	64534
2010.03	858373	17954	39039	74034
2011.05	859766	19769	37646	72219

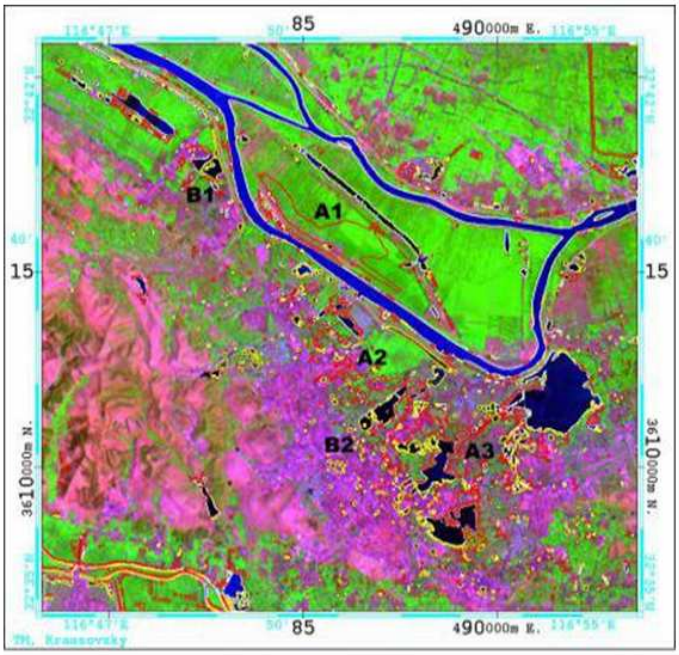

FIGURE 3. Feature fusion image of water body changes in Kongji and Bagong Mountains and Caijiagang district

Area to the Xieyi Mining Area (B2) are both coal gangue landfill areas. Large-area newly-increased pool zones correspond to the ground surface subsidence areas forming in recent years. For example, the displayed locations of A1 (the Erdao River), A2 (the Xinzhuangzi Mine) and A3 (the Xieer Mine) are newly-increased pool zones.

4. **Conclusions.** (1) Remote sensing imaging is selected as data sources and imaging classifications, along with multi-source and multi-temporal imaging fusion techniques, are utilized, which enables one to relatively accurately extract the dynamic change information of coal mining subsidence areas and give full play to the characteristics of the speediness, accuracy and strong periodicity of remote sensing techniques.

(2) Utilizing remote sensing imaging at different periods can also reflect the comprehensive treatment information of subsidence areas and the changing information of land resources, providing reliable basic data for the comprehensive management of the environment in mining areas, which is an effective means for dynamically monitoring the environment in mining areas.

(3) Mining areas are mainly located at the mountain front plain areas, south of the Huai River, where the terrain is gentle and low-lying and groundwater resources are abundant, bringing out relatively large-scale ponding in every coal mining subsidence area. Consequently, further research on the depth and scope of ponding and the changes of water body environments is one significant application of the dynamic evolution monitoring of subsidence areas.

REFERENCES

[1] Y. Sheng, D. Guo and S. Hang, *Industrial Environment Dynamic Monitoring and Analysis*, Geological Publishing House, Beijing, 2001.

[2] S. Peng, L. Wang, Z. Meng et al., Monitoring the seeper subside in coal district by the remote sensing - Examples from Huainan coal district, *Journal of China Coal Society*, vol.27, no.4, pp.374-378, 2002.

[3] L. Chen, *Studies of the Evolution of Monitoring and the Sustainable Utilization of Mining Area Land*, China University of Mining and Technology Press, Xuzhou, 2003.

[4] L. Chen, D. Guo, S. Hu et al., A study on remote sensing monitoring land use change and reclamation measures of subsided land in Xuzhou coal mining area, *Progress in Geography*, vol.23, no.2, pp.10-15, 2004.

[5] Z. Hu, L. Yang and G. Wang, Research on desertification of grassland in prairie coal mine based on remote sensing data – Case study of Huolinhe coal mine, *Journal of China University of Mining & Technology*, vol.34, no.1, pp.6-10, 2005.

[6] L. Wu and W. Shi, On three dimensional geosciences spatial modeling, *Geography and Geo-Information Science*, no.1, 2005.

[7] H. Ma, H. Li, Y. Liu and Y. Wang, Application of D-InSAR technique to the land subsidence monitoring in mining area, *Metal Mline*, no.2, 2011.

[8] Y. Li, Z. Wang and Q. Ma, Precisely investigating and analyzing the mining subsidence based on 3S integrated technology, *Bulletin of Surveying and Mapping*, no.7, 2014.

[9] Z. Qiang and H. Xi, A new data fusion method for improving CBERS-1 IRMSS images based on CCD image, *Remote Sensing for Land & Resources*, no.2, pp.21-25, 2004.

[10] Y. Wu, *Huainan Coal Mining Subsidence Area Dynamic Evolution Simulation and Research on the Effects of Land Use*, China University of Mining and Technology, 2007.

[11] Y. Wu and S. Peng, Land use classification based on chaos immune algorithm and remote sensing image, *Transactions of the CSAE*, vol.23, no.6, pp.154-158, 2007.

[12] Y. Wu, S. Peng, M. Huang et al., Quantitative analysis of water depth in Huainan ponding subsidence based on remote sensing, *Journal of China University of Mining & Technology*, vol.36, no.4, pp.537-541, 2007.

[13] L. Wei, Y. Zhong, L. Zhang and P. Li, Remote sensing image change detection based on multi-band information fusion, *Geomatics and Information Science of Wuhan University*, vol.39, pp.8-11, 2014.

[14] H. Chen, C. Tao, Z. Zou and F. Yu, Automatic urban area extraction using a Gabor filter and high-resolution remote sensing imagery, *Geomatics and Information Science of Wuhan University*, vol.38, no.9, pp.1063-1067, 2013.

[15] X. Cao and C. Ke, Dynamic remote sensing monitoring of land use in Nanjing based on TM images, *Geomatics and Information Science of Wuhan University*, vol.31, no.11, pp.958-961, 2006.

[16] P. M. Atkinson and P. Lewis, Geostatistical classification for remote sensing: An introduction, *Computers & Geosciences*, no.26, pp.361-371, 2000.